**Smart Structures and Systems**, *Vol. 16, No. 3 (2015) 497-519*
DOI: http://dx.doi.org/10.12989/sss.2015.16.3.497 

# Fuzzy modelling approach for shear strength prediction of RC deep beams

Mohammad Mohammadhassani*[1], Aidi MD. Saleh[2b], M Suhatril[3] and M. Safa[3]

*[1]Department of Structural Engineering, University of Malaya, Malaysia*
*[2]Malaysian public work department, Ledang, Tangkak, 84900 Johor, Malaysia*
*[3]Department of Civil Engineering, University of Malaya, Malaysia*

*(Received July 15, 2014, Revised October 24, 2014, Accepted December 30, 2014)*

**Abstract.** This study discusses the use of Adaptive-Network-Based-Fuzzy-Inference-System (ANFIS) in predicting the shear strength of reinforced-concrete deep beams. 139 experimental data have been collected from renowned publications on simply supported high strength concrete deep beams. The results show that the ANFIS has strong potential as a feasible tool for predicting the shear strength of deep beams within the range of the considered input parameters. ANFIS's results are highly accurate, precise and therefore, more satisfactory. Based on the Sensitivity analysis, the shear span to depth ratio (a/d) and concrete cylinder strength ( $f_c'$) have major influence on the shear strength prediction of deep beams. The parametric study confirms the increase in shear strength of deep beams with an equal increase in the concrete strength and decrease in the shear span to-depth-ratio.

**Keywords:** deep beams; ultimate shear strength; ANFIS; LR

## 1. Introduction

Widely used as structural elements, deep beams have various applications. For instance, it is used in transfer girders, foundation walls, offshore structures, pile caps and in nuclear power plant containment structures. Reinforced concrete deep beams are beams with a small shear span-to-depth ratio of less than 2.5, where a significant percentage of the load is transferred to the support through a compression strut that connects both the loading and reaction points.

Numerous studies have been carried out on shear prediction of deep beams. Nielsen (1971) and Braestrup and Nielsen (1981) have used the plasticity concept for the shear strength prediction to resolve deep beam problems. The solutions suggested by these researchers that uses the Strut-and-tie modelling (STM) are found to have better explained the behaviours of deep beam. The STM analyzes deep beams with the plastic truss analogy which internally transfers the load forces from the loading points to the support points through both horizontal and inclined concrete strut and steel reinforcing ties which are acting in tension (Möller *et al.* 2008). Recently published

∗Corresponding author, Dr., E-mail: mmh356@yahoo.com
[a] Independent Researcher
[b] Master of Structural Engineering

**Copyright © 2015 Techno-Press, Ltd.**
http://www.techno-press.org/?journal=sss&subpage=8 ISSN: 1738-1584 (Print), 1738-1991 (Online)

papers by Mohammadhassani *et al*. (2011) have concluded that the behaviour of deep beam and its strain distribution in the height of mid span are difficult to understand and due to their proportions, deep beams are likely to have strength that is controlled by shear.

Smith and Vantsiotis (1982) have taken time to study the shear strength of deep beams to identify the effect of vertical and horizontal web reinforcements and shear span-to-effective depth ratio on the ultimate shear strength. Their results indicate that web reinforcements moderately affect the ultimate shear strength and that the addition of vertical web reinforcement of 0.18 - 1.25% shows significant improvement in the ultimate shear strength of deep beams. Also observed was the considerable increase in the load-carrying capacity when the concrete strength was increased and the shear span-to-effective depth ratio was decreased.

Tan *et al*. (1995) have tested 19 reinforced concrete deep beams with compressive strengths of 41 - 59 MPa under two-point top loading. The beams were tested for seven shear span-depth ratios (*a/d*) from 0.27 - 2.70 and four effective span-depth ratios (*l/d*) from 2.15 - 5.38. The results show that *l/d* has had an insignificant effect on the failure load. Nevertheless, for beams with a/d ≥ 1.00, the flexural failure is dominant with an increasing *l*/d. When compared to the ACI predictions, the results have shown that the ACI code provisions are more suited for deep beams with higher strength. The ACI code is also more conservative compared to the Deep-Beam Design Guide by the Construction Industry Research and Information Association (CIRIA 1997).

Tan *et al*. (1997) have examined the shear prediction on 18 high strength concrete (HSC) deep beams and the results revealed that the ACI Code provisions for deep-beams have overestimated the contribution of the horizontal web steel to shear strength; a revision that has been suggested in the ACI Eqs. (11)-(31) for web steel contribution. They have announced that the Canadian Code, although more consistent, is conservative for deep beams' different web reinforcements, while the UK CIRIA Guide is un-conservative for beams with horizontal web reinforcements.

Tan and Lu (1999) have tested 12 specimens to failure. The beams were tested to study the effect of the beam size on the shear strength of concrete beam. The results have revealed the ultimate shear strength as being size-dependent but the diagonal cracking stress that occurred is not. Compared to current design codes, the CSA is found to be more suitable for large-and medium-sized beams, while both the ACI and CIRIA predictions become less conservative with the increase in the h and a/h ratio.

Oh and Shin (2001), have subsequently studied the shear strength of reinforced HSC deep beams with 53 beams with compressive strengths of 23 - 74 *MPa* and the geometrical variation such as an effective span-depth ratio(le/d) of 3.0 - 5.0 and a shear span-effective depth ratio (a/d) of 0.5 - 2.0. The result has further shown that the ultimate shear strength of deep beams has been determined predominantly by the a/d and that the ACI Code Eqs. (11)-(29) and (11)-(30) are conservative and have underestimated the effects of both the concrete compressive strength ( $f_c'$ ) and the longitudinal steel reinforcement ( $\rho_t$ ).

Yang *et al.* (2003) have conducted a test on 21 beam specimens to investigate their shear characteristics as concrete strengths, shear span/depth ratios, and overall depths. Based on their findings, the decrease in the shear span/depth ratio and the increase in overall depth while the shear span/depth ratio remains unchanged, have led to more brittle failures with wide diagonal cracks and high energy release. The ACI code has given similar safety factors on the shear strength when the first diagonal crack appears, but it does not specify a maximum limit for the safety factor in terms of the ultimate strength and the effect of the beam size.

More recent studies on deep beam behaviour have been carried out by Mohammadhassani

(2011a) and Lu *et al.* (2010) but none has defined the exact shear prediction for deep beams. A comprehensive literature review was carried out on this matter and many parameters have been identified to affect the shear strength of deep beams. Amongst them are the concrete compressive strength, web reinforcement percentages, tensile reinforcement ratio, length and shear span to depth ratio (Yang *et al*. 2006).

With the ever increasing costs of casting, curing and testing of deep beams, the search for new inexpensive effective tools for the design of deep beams has intensified which is achievable through the modelling and determination of its shear capacity. This involves the use of classical and /or modern analytical models to predict the ultimate shear strength of the deep beam with emphasis on its behaviour and the non-linear strain distribution.

The Artificial Intelligence (AI) system approaches such as the Fuzzy Inference Systems (FIS), Neuro-Fuzzy (NF)/ Fuzzy-Neural (FN) and Artificial Neural Network(ANN) systems have paved the way for successful modelling of many engineering applications as well as in other fields such as hydraulic engineering (Shatirah *et al*. 2014), Rainfall Forecasting (Akrami *et al*. 2013), the stability of structures (Bilgehan 2011) and deflection prediction of deep beams (Mohammadhassani *et al.* 2013).

The AI is an established tool for pattern recognition, signal processing and control and complex mapping, mainly due to its excellent learning capacity and high error tolerance (Kao and Hung. 2011).

The use of the AI technique in Civil Engineering began when ANN was used to predict the ultimate shear strength of reinforced concrete deep beams where Sanad and Saka (2001) have shown that the shear strengths of normal beams and deep beams are better predicted using multi-layered feed forward ANNs than other existing formulas.

Fuzzy logic systems are more suited for the modelling of the relationship between variables in environments that are either ill-defined or very complex, yet still produce a more precise alternative. The use of qualitative variables and mathematical relationships in this technique is more accurate in the decision-making process (Khaleie and Fasanghari 2012). First introduced by Zadeh (1965), fuzzy logic is a self-learning technique which has a mathematical tool to convert linguistic evaluation variables based on expert knowledge into an automatic evaluation strategy.

The ANFIS is a fuzzy-neural system which is a combination of significant characteristics of ANNs and fuzzy inference system (FIS) for computing. The ANFIS uses the ANN theory in order to determine the fuzzy membership functions and fuzzy rules properties of data samples in learning a fuzzy inference system which is based on the Takagi-Sugeno fuzzy model (Takagi and Sugeno 1985). With the ANFIS, a fuzzy inference system is implemented with a feed-forward network and a hybrid learning method including the back propagation theory from ANNs, the recursive least square (RLS) method and clustering techniques. All the aforementioned are used together to construct the FIS accordingly for the data. In other words, the ANFIS combines the fuzzy logic and ANNs by using the mathematical properties of ANNs in the tuning rule-based fuzzy inference system that emulates the way human brain processes information. The ANFIS shows a significant promise in modeling nonlinear systems, as it has the ability to learn features of the data set and adjust accordingly the system characteristics to a given error criterion (Jang 1993). Also, the ANFIS can map unseen inputs to their outputs by learning the rules from previously seen data.

Due to the aforesaid ability and advantages, the ANFIS is increasingly becoming popular in the modern world in different fields of engineering (Lin *et al.* 1996).

This research examines the ANFIS and its applications in the prediction of shear strength of concrete deep beams.

### *1.1 Review on related works*

Mashrei *et al*. (2010) have presented the results of the back-propagation neural networks (BPNN) and an adaptive neuro-fuzzy inference system (ANFIS) models in predicting the moment capacity of ferro-cement members. The selected input variables have included the width and depth of specimens, the cube compressive strength of mortar, and tensile strength and volume fraction of wire mesh to study the influence of each parameter on the moment capacity of the ferro-cement member. The results have demonstrated that both the BPNN and ANFIS provide good predictions compared to other available methods.

Bilgehan (2011) have used the ANFIS and ANN models to analyse the buckling in slender prismatic columns with a single non-propagating open edge crack under axial loads. The main focus was to study the feasibility of using the ANFIS and ANN trained with the non-dimensional crack depth and the non-dimensional crack location parameters to predict the critical buckling load of different ends-supported condition in axially loaded compression rods. The conclusion is that the ANFIS architecture with the Gaussian membership function performs relatively better than the multilayer feed forward ANN learning by the back propagation algorithm.

### *1.2 Research significance*

This paper presents and compares the effectiveness of ANFIS and linear regression (LR) in the prediction of the ultimate shear strength in reinforced concrete deep beams. The shear strength, crack development and crack widths are major concerns in the design of deep beam. For the first time ever, an ANFIS model is built, trained and tested using the available test data of 139 deep beams collected from technical literature. The proposed model can adequately predict the ultimate shear strength of deep beams at different tensile reinforcement ratios, web bar percentages, compressive strengths of concrete, yield and ultimate strength of reinforcement and shear span-to-depth ratios. This paper is presented in the following order: Section 2; Dataset used, Section 3; system modelling, Section 4; Results and Discussion and Section 5; Conclusion.

## 2. Methodology

### *2.1 Dataset used*

The experimental data from published works (pal and Deswal 2011), (Zang and Tan 2007) and (Yang *et al.* 2003)) are used to study the effectiveness of the ANFIS in the shear strength prediction of deep beams. These include experimental data from 139 reinforced deep beams of which 19 are HSC-reinforced deep beams from (Tan *et al.* 1995) , 52 from (Smith and Vantsiotis 1982), 35 from (Kong *et al*. 1970), 21 from (Zhang and Tan 2007) and 12 from (Yang *et al*. 2003). The complete dataset is provided in Table 1 and the shear strength unit is expressed in kN.

The datasets of different parameters used in the ANFIS model are presented in Table 2.

Table 1 Datasets of published works

| $l/d$ | $d/b_w$ | $a/d$ | $f'_c$ | $f_{yh}$ | $f_{yv}$ | $\rho_h$ | $\rho_s$ | $\rho_v$ | $V_{exp}$ | $\frac{V_{exp}}{V_{ANFIS}}$ | $\frac{V_{exp}}{V_{LR}}$ |
|---|---|---|---|---|---|---|---|---|---|---|---|
| 19 High strength concrete deep beam(Tan *et al*. 1995) | | | | | | | | | | | |
| 2.15 | 4.21 | 0.27 | 0.0588 | 0.505 | 0.375 | 0.000 | 0.012 | 0.005 | 675 | 1.36 | 1.63 |
| 3.23 | 4.21 | 0.27 | 0.0516 | 0.505 | 0.375 | 0.000 | 0.012 | 0.005 | 630 | 1.00 | 1.34 |
| 4.3 | 4.21 | 0.27 | 0.0539 | 0.505 | 0.375 | 0.000 | 0.012 | 0.005 | 640 | 1.00 | 1.22 |
| 5.38 | 4.21 | 0.27 | 0.0573 | 0.505 | 0.375 | 0.000 | 0.012 | 0.005 | 630 | 1.00 | 1.09 |
| 2.15 | 4.21 | 0.54 | 0.0560 | 0.505 | 0.375 | 0.000 | 0.012 | 0.005 | 468 | 1.00 | 1.38 |
| 3.23 | 4.21 | 0.54 | 0.0457 | 0.505 | 0.375 | 0.000 | 0.012 | 0.005 | 445 | 1.00 | 1.13 |
| 4.3 | 4.21 | 0.54 | 0.0539 | 0.505 | 0.375 | 0.000 | 0.012 | 0.005 | 500 | 0.84 | 1.12 |
| 5.38 | 4.21 | 0.54 | 0.0530 | 0.505 | 0.375 | 0.000 | 0.012 | 0.005 | 480 | 1.00 | 0.95 |
| 2.15 | 4.21 | 0.81 | 0.0512 | 0.505 | 0.375 | 0.000 | 0.012 | 0.005 | 403 | 1.19 | 1.54 |
| 3.23 | 4.21 | 0.81 | 0.0440 | 0.505 | 0.375 | 0.000 | 0.012 | 0.005 | 400 | 1.18 | 1.26 |
| 2.15 | 4.21 | 1.08 | 0.0482 | 0.505 | 0.375 | 0.000 | 0.012 | 0.005 | 270 | 1.00 | 1.45 |
| 3.23 | 4.21 | 1.08 | 0.0441 | 0.505 | 0.375 | 0.000 | 0.012 | 0.005 | 280 | 1.00 | 1.16 |
| 4.3 | 4.21 | 1.08 | 0.0468 | 0.505 | 0.375 | 0.000 | 0.012 | 0.005 | 290 | 1.22 | 0.98 |
| 5.38 | 4.21 | 1.08 | 0.0480 | 0.505 | 0.375 | 0.000 | 0.012 | 0.005 | 290 | 1.00 | 0.83 |
| 'Table 1, continued'. | | | | | | | | | | | |
| 3.23 | 4.21 | 1.62 | 0.0506 | 0.505 | 0.375 | 0.000 | 0.012 | 0.005 | 220 | 1.00 | 2.49 |
| 4.3 | 4.21 | 1.62 | 0.0446 | 0.505 | 0.375 | 0.000 | 0.012 | 0.005 | 190 | 1.00 | 1.33 |
| 5.38 | 4.21 | 1.62 | 0.0453 | 0.505 | 0.375 | 0.000 | 0.012 | 0.005 | 173 | 1.00 | 0.87 |
| 4.3 | 4.21 | 2.16 | 0.0411 | 0.505 | 0.375 | 0.000 | 0.012 | 0.005 | 150 | 1.00 | -16.13 |
| 5.38 | 4.21 | 2.7 | 0.0428 | 0.505 | 0.375 | 0.000 | 0.012 | 0.005 | 107 | 1.00 | -1.00 |
| 52 Normal strength concrete deep beam(Smith and Vantsiotis 1982) | | | | | | | | | | | |
| 2.67 | 2.99 | 1 | 0.0205 | 0.484 | 0.484 | 0.000 | 0.019 | 0.000 | 140 | 1.00 | 0.50 |
| 2.67 | 2.99 | 1 | 0.0209 | 0.484 | 0.484 | 0.000 | 0.019 | 0.000 | 136 | 0.97 | 0.48 |
| 2.67 | 2.99 | 1 | 0.0187 | 0.484 | 0.484 | 0.002 | 0.019 | 0.003 | 161 | 1.00 | 0.64 |
| 2.67 | 2.99 | 1 | 0.0180 | 0.484 | 0.484 | 0.005 | 0.019 | 0.003 | 149 | 1.00 | 0.63 |
| 2.67 | 2.99 | 1 | 0.0161 | 0.484 | 0.484 | 0.007 | 0.019 | 0.003 | 141 | 1.00 | 0.65 |
| 2.67 | 2.99 | 1 | 0.0206 | 0.484 | 0.484 | 0.007 | 0.019 | 0.003 | 171 | 1.00 | 0.79 |

Continued-

| | | | | | | | | | | | |
|---|---|---|---|---|---|---|---|---|---|---|---|
| 2.67 | 2.99 | 1 | 0.0211 | 0.484 | 0.484 | 0.009 | 0.019 | 0.003 | 184 | 1.10 | 0.92 |
| 2.67 | 2.99 | 1 | 0.0217 | 0.484 | 0.484 | 0.002 | 0.019 | 0.006 | 175 | 1.07 | 0.75 |
| 2.67 | 2.99 | 1 | 0.0198 | 0.484 | 0.484 | 0.005 | 0.019 | 0.006 | 171 | 1.00 | 0.78 |
| 2.67 | 2.99 | 1 | 0.0203 | 0.484 | 0.484 | 0.007 | 0.019 | 0.006 | 172 | 1.00 | 0.86 |
| 2.67 | 2.99 | 1 | 0.0191 | 0.484 | 0.484 | 0.009 | 0.019 | 0.006 | 162 | 1.00 | 0.88 |
| 2.67 | 2.99 | 1 | 0.0181 | 0.484 | 0.484 | 0.002 | 0.019 | 0.013 | 161 | 1.12 | 0.78 |
| 2.67 | 2.99 | 1 | 0.0192 | 0.484 | 0.484 | 0.005 | 0.019 | 0.013 | 173 | 1.00 | 0.92 |
| 2.67 | 2.99 | 1 | 0.0208 | 0.484 | 0.484 | 0.007 | 0.019 | 0.013 | 179 | 1.00 | 1.04 |
| 2.67 | 2.99 | 1 | 0.0199 | 0.484 | 0.484 | 0.009 | 0.019 | 0.013 | 168 | 1.00 | 1.09 |
| 3.08 | 2.99 | 1.21 | 0.0217 | 0.484 | 0.484 | 0.000 | 0.019 | 0.000 | 149 | 1.04 | 0.61 |
| 3.08 | 2.99 | 1.21 | 0.0221 | 0.484 | 0.484 | 0.002 | 0.019 | 0.002 | 148 | 1.00 | 0.69 |
| 3.08 | 2.99 | 1.21 | 0.0201 | 0.484 | 0.484 | 0.005 | 0.019 | 0.002 | 144 | 1.14 | 0.73 |
| 3.08 | 2.99 | 1.21 | 0.0208 | 0.484 | 0.484 | 0.007 | 0.019 | 0.002 | 141 | 1.00 | 0.78 |
| 3.08 | 2.99 | 1.21 | 0.0195 | 0.484 | 0.484 | 0.009 | 0.019 | 0.002 | 154 | 1.00 | 0.94 |
| 'Table 1, continued'. | | | | | | | | | | | |
| 3.08 | 2.99 | 1.21 | 0.0192 | 0.484 | 0.484 | 0.002 | 0.019 | 0.004 | 129 | 1.00 | 0.62 |
| 3.08 | 2.99 | 1.21 | 0.0190 | 0.484 | 0.484 | 0.005 | 0.019 | 0.004 | 131 | 1.00 | 0.69 |
| 3.08 | 2.99 | 1.21 | 0.0175 | 0.484 | 0.484 | 0.007 | 0.019 | 0.004 | 126 | 1.00 | 0.73 |
| 3.08 | 2.99 | 1.21 | 0.0218 | 0.484 | 0.484 | 0.007 | 0.019 | 0.004 | 150 | 1.00 | 0.87 |
| 3.08 | 2.99 | 1.21 | 0.0198 | 0.484 | 0.484 | 0.009 | 0.019 | 0.004 | 145 | 1.00 | 0.93 |
| 3.08 | 2.99 | 1.21 | 0.0162 | 0.484 | 0.484 | 0.002 | 0.019 | 0.006 | 131 | 0.93 | 0.67 |
| 3.08 | 2.99 | 1.21 | 0.0204 | 0.484 | 0.484 | 0.002 | 0.019 | 0.008 | 159 | 1.00 | 0.84 |
| 3.08 | 2.99 | 1.21 | 0.0190 | 0.484 | 0.484 | 0.005 | 0.019 | 0.008 | 159 | 0.98 | 0.92 |
| 3.08 | 2.99 | 1.21 | 0.0192 | 0.484 | 0.484 | 0.007 | 0.019 | 0.008 | 155 | 1.00 | 0.99 |
| 3.08 | 2.99 | 1.21 | 0.0207 | 0.484 | 0.484 | 0.009 | 0.019 | 0.008 | 166 | 1.00 | 1.20 |
| 3.08 | 2.99 | 1.21 | 0.0171 | 0.484 | 0.484 | 0.002 | 0.019 | 0.013 | 154 | 1.00 | 0.92 |
| 3.67 | 2.99 | 1.5 | 0.0207 | 0.484 | 0.484 | 0.000 | 0.019 | 0.000 | 116 | 0.48 | 0.60 |
| 3.67 | 2.99 | 1.5 | 0.0192 | 0.484 | 0.484 | 0.002 | 0.019 | 0.002 | 119 | 1.00 | 0.72 |
| 3.67 | 2.99 | 1.5 | 0.0219 | 0.484 | 0.484 | 0.005 | 0.019 | 0.002 | 124 | 1.00 | 0.83 |
| 3.67 | 2.99 | 1.5 | 0.0227 | 0.484 | 0.484 | 0.007 | 0.019 | 0.002 | 131 | 1.00 | 0.99 |

Continued-

| | | | | | | | | | | | |
|---|---|---|---|---|---|---|---|---|---|---|---|
| 3.67 | 2.99 | 1.5 | 0.0218 | 0.484 | 0.484 | 0.009 | 0.019 | 0.002 | 123 | 1.00 | 1.07 |
| 3.67 | 2.99 | 1.5 | 0.0199 | 0.484 | 0.484 | 0.002 | 0.019 | 0.003 | 124 | 1.00 | 0.77 |
| 3.67 | 2.99 | 1.5 | 0.0192 | 0.484 | 0.484 | 0.005 | 0.019 | 0.003 | 104 | 1.00 | 0.73 |
| 3.67 | 2.99 | 1.5 | 0.0193 | 0.484 | 0.484 | 0.005 | 0.019 | 0.003 | 116 | 1.00 | 0.81 |
| 3.67 | 2.99 | 1.5 | 0.0204 | 0.484 | 0.484 | 0.007 | 0.019 | 0.003 | 125 | 1.00 | 0.99 |
| 3.67 | 2.99 | 1.5 | 0.0208 | 0.484 | 0.484 | 0.009 | 0.019 | 0.003 | 124 | 1.00 | 1.14 |
| 3.67 | 2.99 | 1.5 | 0.0210 | 0.484 | 0.484 | 0.002 | 0.019 | 0.006 | 141 | 1.00 | 0.95 |
| 3.67 | 2.99 | 1.5 | 0.0166 | 0.484 | 0.484 | 0.005 | 0.019 | 0.006 | 125 | 1.00 | 0.95 |
| 3.67 | 2.99 | 1.5 | 0.0183 | 0.484 | 0.484 | 0.007 | 0.019 | 0.006 | 128 | 1.00 | 1.12 |
| 3.67 | 2.99 | 1.5 | 0.0190 | 0.484 | 0.484 | 0.009 | 0.019 | 0.006 | 137 | 1.00 | 1.42 |
| 3.67 | 2.99 | 1.5 | 0.0196 | 0.484 | 0.484 | 0.002 | 0.019 | 0.008 | 147 | 1.00 | 1.06 |
| 'Table 1, continued'. | | | | | | | | | | | |
| 3.67 | 2.99 | 1.5 | 0.0186 | 0.484 | 0.484 | 0.005 | 0.019 | 0.006 | 129 | 1.00 | 1.01 |
| 3.67 | 2.99 | 1.5 | 0.0192 | 0.484 | 0.484 | 0.005 | 0.019 | 0.008 | 153 | 1.00 | 1.26 |
| 3.67 | 2.99 | 1.5 | 0.0185 | 0.484 | 0.484 | 0.007 | 0.019 | 0.008 | 153 | 1.00 | 1.47 |
| 3.67 | 2.99 | 1.5 | 0.0212 | 0.484 | 0.484 | 0.009 | 0.019 | 0.008 | 160 | 1.00 | 1.84 |
| 4.83 | 2.99 | 2.08 | 0.0195 | 0.484 | 0.484 | 0.000 | 0.019 | 0.000 | 47 | 1.00 | 0.54 |
| 4.83 | 2.99 | 2.08 | 0.0161 | 0.484 | 0.484 | 0.002 | 0.019 | 0.004 | 88 | 1.00 | 1.74 |
| 35 Normal strength concrete deep beam (Kong *et al.* 1970) | | | | | | | | | | | |
| 1.05 | 9.53 | 0.35 | 0.0215 | 0.000 | 0.028 | 0.000 | 0.000 | 0.025 | 239 | 1.07 | 1.00 |
| 1.28 | 7.86 | 0.43 | 0.0246 | 0.000 | 0.028 | 0.000 | 0.000 | 0.025 | 224 | 1.00 | 1.04 |
| 1.62 | 6.18 | 0.54 | 0.0212 | 0.000 | 0.028 | 0.000 | 0.000 | 0.025 | 190 | 1.00 | 1.00 |
| 2.22 | 4.51 | 0.74 | 0.0212 | 0.000 | 0.028 | 0.000 | 0.000 | 0.025 | 164 | 1.00 | 1.08 |
| 3.53 | 2.84 | 1.18 | 0.0217 | 0.000 | 0.028 | 0.000 | 0.000 | 0.025 | 90 | 1.00 | 1.09 |
| 1.05 | 9.53 | 0.35 | 0.0192 | 0.000 | 0.303 | 0.000 | 0.000 | 0.009 | 249 | 1.14 | 0.71 |
| 1.28 | 7.86 | 0.43 | 0.0186 | 0.000 | 0.303 | 0.000 | 0.000 | 0.009 | 224 | 1.00 | 0.69 |
| 1.62 | 6.18 | 0.54 | 0.0199 | 0.000 | 0.303 | 0.000 | 0.000 | 0.009 | 216 | 1.01 | 0.72 |
| 2.22 | 4.51 | 0.74 | 0.0228 | 0.000 | 0.303 | 0.000 | 0.000 | 0.009 | 140 | 1.00 | 0.53 |
| 3.53 | 2.84 | 1.18 | 0.0201 | 0.000 | 0.303 | 0.000 | 0.000 | 0.009 | 100 | 1.00 | 0.52 |
| 1.05 | 9.53 | 0.35 | 0.0226 | 0.280 | 0.000 | 0.025 | 0.000 | 0.000 | 276 | 1.00 | 1.86 |

Continued-

| | | | | | | | | | | | |
|---|---|---|---|---|---|---|---|---|---|---|---|
| 1.28 | 7.86 | 0.43 | 0.0210 | 0.280 | 0.000 | 0.025 | 0.000 | 0.000 | 226 | 1.00 | 1.81 |
| 1.62 | 6.18 | 0.54 | 0.0192 | 0.280 | 0.000 | 0.025 | 0.000 | 0.000 | 208 | 1.00 | 2.10 |
| 2.22 | 4.51 | 0.74 | 0.0219 | 0.280 | 0.000 | 0.025 | 0.000 | 0.000 | 159 | 0.75 | 2.61 |
| 3.53 | 2.84 | 1.18 | 0.0226 | 0.280 | 0.000 | 0.025 | 0.000 | 0.000 | 87 | 1.00 | -1.01 |
| 1.05 | 9.53 | 0.35 | 0.0220 | 0.303 | 0.000 | 0.009 | 0.000 | 0.000 | 242 | 1.00 | 0.91 |
| 1.28 | 7.86 | 0.43 | 0.0210 | 0.303 | 0.000 | 0.009 | 0.000 | 0.000 | 201 | 1.00 | 0.82 |
| 1.62 | 6.18 | 0.54 | 0.0201 | 0.303 | 0.000 | 0.009 | 0.000 | 0.000 | 181 | 0.75 | 0.83 |
| 2.22 | 4.51 | 0.74 | 0.0220 | 0.303 | 0.000 | 0.009 | 0.000 | 0.000 | 110 | 1.00 | 0.61 |
| 'Table 1, continued'. | | | | | | | | | | | |
| 3.53 | 2.84 | 1.18 | 0.0226 | 0.303 | 0.000 | 0.009 | 0.000 | 0.000 | 96 | 1.00 | 0.87 |
| 1.05 | 9.53 | 0.35 | 0.0186 | 0.280 | 0.280 | 0.006 | 0.000 | 0.006 | 240 | 1.00 | 0.82 |
| 1.28 | 7.86 | 0.43 | 0.0192 | 0.280 | 0.280 | 0.006 | 0.000 | 0.006 | 208 | 1.00 | 0.77 |
| 1.62 | 6.18 | 0.54 | 0.0201 | 0.280 | 0.280 | 0.006 | 0.000 | 0.006 | 173 | 1.00 | 0.71 |
| 2.22 | 4.51 | 0.74 | 0.0219 | 0.280 | 0.280 | 0.006 | 0.000 | 0.006 | 127 | 1.00 | 0.62 |
| 3.53 | 2.84 | 1.18 | 0.0226 | 0.280 | 0.280 | 0.006 | 0.000 | 0.006 | 78 | 0.46 | 0.57 |
| 1.05 | 9.53 | 0.35 | 0.0261 | 0.303 | 0.000 | 0.005 | 0.000 | 0.000 | 308 | 1.23 | 1.05 |
| 1.28 | 7.86 | 0.43 | 0.0251 | 0.303 | 0.000 | 0.006 | 0.000 | 0.000 | 266 | 1.00 | 1.01 |
| 1.62 | 6.18 | 0.54 | 0.0261 | 0.303 | 0.000 | 0.008 | 0.000 | 0.000 | 245 | 1.00 | 1.09 |
| 2.22 | 4.51 | 0.74 | 0.0261 | 0.303 | 0.000 | 0.010 | 0.000 | 0.000 | 173 | 1.00 | 1.03 |
| 3.53 | 2.84 | 1.18 | 0.0251 | 0.303 | 0.000 | 0.015 | 0.000 | 0.000 | 99 | 1.00 | 1.66 |
| 1.05 | 10.03 | 0.35 | 0.0251 | 0.303 | 0.000 | 0.000 | 0.000 | 0.000 | 253 | 0.76 | 0.75 |
| 1.05 | 10.03 | 0.35 | 0.0261 | 0.303 | 0.000 | 0.002 | 0.000 | 0.000 | 300 | 1.00 | 0.93 |
| 1.05 | 10.03 | 0.35 | 0.0251 | 0.303 | 0.000 | 0.003 | 0.000 | 0.000 | 260 | 1.00 | 0.84 |
| 1.05 | 10.03 | 0.35 | 0.0213 | 0.303 | 0.000 | 0.007 | 0.000 | 0.000 | 264 | 0.84 | 0.93 |
| 1.05 | 10.03 | 0.35 | 0.0213 | 0.303 | 0.000 | 0.009 | 0.000 | 0.000 | 297 | 1.00 | 1.09 |
| 21 concrete Deep beams (Zhang and Tan 2007) | | | | | | | | | | | |
| 3.35 | 3.91 | 1.1 | 0.0259 | 0.000 | 0.426 | 0.000 | 0.013 | 0.005 | 99.5 | 1.00 | 0.35 |
| 3.3 | 3.95 | 1.1 | 0.0274 | 0.000 | 0.426 | 0.000 | 0.013 | 0.003 | 186.5 | 1.00 | 0.65 |
| 3.27 | 4.01 | 1.1 | 0.0283 | 0.000 | 0.370 | 0.000 | 0.012 | 0.004 | 427 | 1.00 | 1.57 |
| 3.32 | 3.93 | 1.1 | 0.0287 | 0.000 | 0.455 | 0.000 | 0.012 | 0.005 | 775 | 1.00 | 2.75 |

Continued-

| | | | | | | | | | | | |
|---|---|---|---|---|---|---|---|---|---|---|---|
| 3.34 | 3.93 | 1.1 | 0.0274 | 0.000 | 0.000 | 0.000 | 0.013 | 0.000 | 85 | 1.00 | 0.34 |
| 3.27 | 5.74 | 1.1 | 0.0324 | 0.000 | 0.000 | 0.000 | 0.012 | 0.000 | 135.5 | 1.00 | 0.53 |
| 3.23 | 8.13 | 1.1 | 0.0248 | 0.000 | 0.000 | 0.000 | 0.013 | 0.000 | 155.5 | 1.00 | 0.56 |
| 3.24 | 11.58 | 1.1 | 0.0306 | 0.000 | 0.000 | 0.000 | 0.013 | 0.000 | 241.5 | 1.00 | 0.80 |
| 3.34 | 3.93 | 1.1 | 0.0274 | 0.000 | 0.000 | 0.000 | 0.013 | 0.000 | 85 | 1.00 | 0.34 |
| ‘Table 1, continued’. | | | | | | | | | | | |
| 3.3 | 3.95 | 1.1 | 0.0283 | 0.000 | 0.000 | 0.000 | 0.013 | 0.000 | 167 | 1.00 | 0.67 |
| 3.27 | 4.01 | 1.1 | 0.0287 | 0.000 | 0.000 | 0.000 | 0.012 | 0.000 | 360.5 | 1.00 | 1.47 |
| 3.32 | 3.93 | 1.1 | 0.0293 | 0.000 | 0.000 | 0.000 | 0.012 | 0.000 | 672 | 1.00 | 2.72 |
| 2.82 | 2.22 | 0.56 | 0.0314 | 0.000 | 0.000 | 0.000 | 0.010 | 0.000 | 446.9 | 1.00 | 0.90 |
| 3.78 | 3.47 | 0.54 | 0.0314 | 0.000 | 0.000 | 0.000 | 0.010 | 0.000 | 535.1 | 1.00 | 0.96 |
| 2.7 | 3.47 | 0.54 | 0.0314 | 0.000 | 0.000 | 0.000 | 0.010 | 0.000 | 479.2 | 1.00 | 0.95 |
| 1.97 | 4.28 | 0.55 | 0.0314 | 0.000 | 0.000 | 0.000 | 0.010 | 0.000 | 596.8 | 1.09 | 1.27 |
| 1.71 | 5.84 | 0.53 | 0.0314 | 0.000 | 0.000 | 0.000 | 0.009 | 0.000 | 582.1 | 1.00 | 1.24 |
| 3.94 | 2.22 | 1.13 | 0.0314 | 0.000 | 0.000 | 0.000 | 0.010 | 0.000 | 192.1 | 0.76 | 0.49 |
| 3.94 | 2.22 | 1.13 | 0.0314 | 0.000 | 0.000 | 0.000 | 0.010 | 0.000 | 311.6 | 1.24 | 0.80 |
| 3.78 | 3.47 | 1.08 | 0.0314 | 0.000 | 0.000 | 0.000 | 0.010 | 0.000 | 375.3 | 0.47 | 0.92 |
| 3.066 | 4.28 | 1.09 | 0.0314 | 0.000 | 0.000 | 0.000 | 0.010 | 0.000 | 271.5 | 0.90 | 0.73 |
| 3.066 | 4.28 | 1.09 | 0.0314 | 0.000 | 0.000 | 0.000 | 0.010 | 0.000 | 330.3 | 1.10 | 0.89 |
| 2.78 | 5.84 | 1.07 | 0.0314 | 0.000 | 0.000 | 0.000 | 0.009 | 0.000 | 543.9 | 1.00 | 2.19 |
| 2.82 | 2.22 | 0.56 | 0.0785 | 0.000 | 0.000 | 0.000 | 0.010 | 0.000 | 733 | 0.94 | 1.04 |
| 3.78 | 3.47 | 0.54 | 0.0785 | 0.000 | 0.000 | 0.000 | 0.010 | 0.000 | 823.2 | 1.00 | 1.07 |
| 1.97 | 4.28 | 0.55 | 0.0785 | 0.000 | 0.000 | 0.000 | 0.010 | 0.000 | 1010.4 | 1.02 | 1.49 |
| 1.71 | 5.84 | 0.53 | 0.0785 | 0.000 | 0.000 | 0.000 | 0.009 | 0.000 | 1029 | 1.00 | 1.52 |
| 3.94 | 2.22 | 1.13 | 0.0785 | 0.000 | 0.000 | 0.000 | 0.010 | 0.000 | 498.8 | 1.13 | 0.83 |
| 3.94 | 2.22 | 1.13 | 0.0785 | 0.000 | 0.000 | 0.000 | 0.010 | 0.000 | 385.1 | 0.87 | 0.64 |
| 3.78 | 3.47 | 1.08 | 0.0785 | 0.000 | 0.000 | 0.000 | 0.010 | 0.000 | 573.3 | 1.00 | 0.93 |
| 3.06 | 4.28 | 1.09 | 0.0785 | 0.000 | 0.000 | 0.000 | 0.010 | 0.000 | 338.1 | 0.97 | 0.58 |
| 3.06 | 4.28 | 1.09 | 0.0785 | 0.000 | 0.000 | 0.000 | 0.010 | 0.000 | 360.6 | 1.03 | 0.62 |
| 2.78 | 5.84 | 1.07 | 0.0785 | 0.000 | 0.000 | 0.000 | 0.009 | 0.000 | 769.3 | 1.00 | 1.32 |

Table 2 Different parameters of the deep beams dataset

| Input Parameters | | | | | | | | | Output |
|---|---|---|---|---|---|---|---|---|---|
| $l/d$ | $d/b_w$ | $a/d$ | $f_c'$ | $f_{yh}$ | $f_{yv}$ | $\rho_h$ | $\rho_s$ | $\rho_v$ | $V_{\exp}$ |

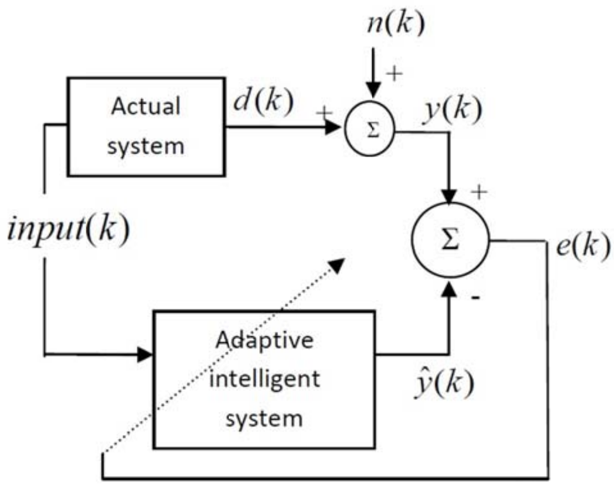


Fig. 1 System modelling using an adaptive intelligent system (Mohammadhassani 2013a)

where:

*L/d = effective span to effective depth ratio*

$f_c'$ *= concrete compressive strength*

*d/b*$_w$*= effective depth to breadth ratio,*

*a/d= shear span to effective depth ratio*

$f_{yh}$*=yield strength of horizontal reinforcement,*

$f_{yv}$*= yield strength of vertical web reinforcement,*

$\rho_h$ *= horizontal web reinforcement ratio*

$\rho_s =$ *longitudinal reinforcement area to area of concrete ratio*

$\rho_v$ *= vertical web reinforcement (qv) ratio*

*when shear strength ($V_{exp}$) is used as the output.*

### 2.2 System modeling (Mohammadhassani 2013a)

System modeling alters the parameters of an adaptive intelligent system such as ANFIS to suit unknown real life engineering system transfer function. A schematic of a problem modeling system using adaptive intelligent system is shown in Fig. 1; the parameters are tuned through proper learning methods to ensure more accurate estimation of the actual system. In other words, the performance function which typically is the mean squared error (MSE) between an intelligent system's output and actual response is minimized.

The objective function in a problem modelling system is as follows

$$MSE = \frac{1}{L}\sum_{k=1}^{L}(\hat{y}(k) - y(k))^2 \tag{1}$$

where $y(k)$ is noisy output of a real life system (measured or observed output), $\hat{y}(k)$ is the adaptive intelligent system's output and $L$ is the number of instances. In cases that are noise free, $y(k)$ is equal to $d(k)$ and this is the desired output. If noise is present, $\hat{y}(k)$ is the estimation of desired output or semi desired output.

### *2.2.1 Fuzzy expert system (Mohammadhassani 2013a)*

Human reasoning is able to process uncertainties and vague concepts appropriately. It cannot however, express them precisely. Fuzzy logic enables the modelling of uncertainties and the human brain's way of thinking, reasoning and perception. Using the Boolean logic, two concepts are applied, 'TRUE' or 'FALSE', and they are represented by 1 and 0 respectively; a proposition can only be true or false. As an extension of the Boolean logic, fuzzy logic allows intermediate values between 1 and 0 where the classical theory of binary membership in a set has been extended to incorporate memberships between 0 and 1. This extension allows each proposition to be to a certain degree of TRUE or FALSE. Using $X$ as the space of objects and $x$ as an element of $X$, the classical A set, $A \subseteq X$, is defined as a collection of elements $x \in X$, where $x$ can either belong or not belong to the set $A$ which is as described in Eq. (2).

$$A = \{x | x \in X\} \tag{2}$$

whereas, a fuzzy set $A$ in $X$ is defined by Eq. (3)

$$A = \{(x, \mu_A(x)) | x \in X\} \tag{3}$$

$\mu_A(x)$ is the membership function for the fuzzy set A, where $A$ is a linguistic term (label) determined by the fuzzy set. The membership function maps each $x$ element to a membership grade between 0 and 1 where $(\mu_A(x) \in [0,1])$. For example, this set can present $x$ as 'Medium', which is described by a fuzzy set with soft boundaries. Fig. 2 shows both (a) the Boolean logic and (b) the fuzzy logic sets.

### *2.2.2 Fuzzy Inference System (FIS) (Mohammadhassani 2013a)*

Fuzzy systems offer the means of representing the expert knowledge of human brain processes in terms of fuzzy (IF–THEN) rules as a basic unit for the capturing of knowledge in a fuzzy system. The fuzzy rule has two components: 'IF' and 'THEN'; these components are known as antecedent and consequent, respectively. The main structure of the fuzzy rule is shown in Eq. (4)

*IF* <antecedent> *THEN* <consequent> (4)

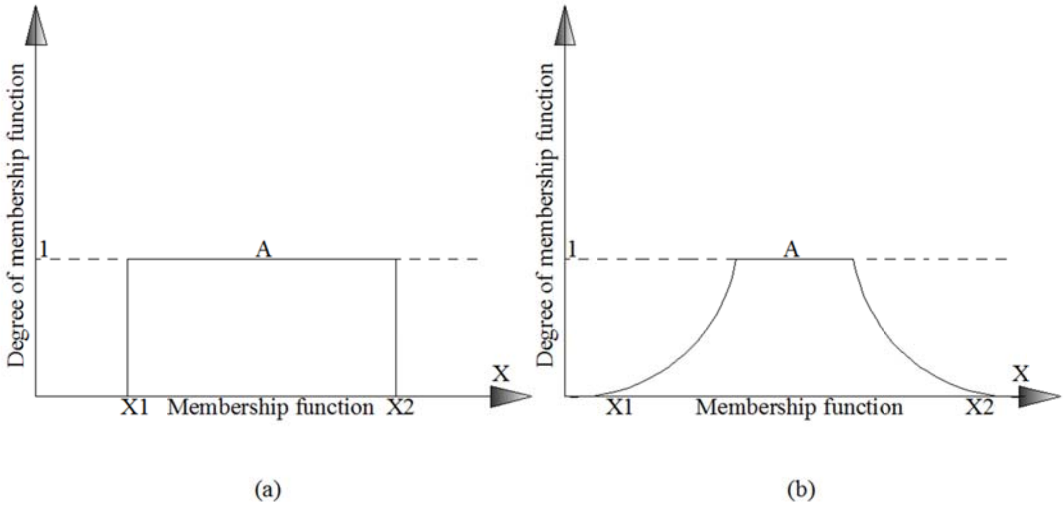


Fig. 2 Examples of: (a) Classical Boolean set, and (b) Fuzzy Logic set (Mohammadhassani 2013a)

Conditionally, the antecedent of a fuzzy rule can be satisfied to a degree. Similar to conventional rules, the antecedent of a fuzzy rule can combine multiple simple conditions into a complex string using AND, OR and NOT logic operators. The consequence of a fuzzy rule is classified into two main categories:

a) Fuzzy consequent (Eq. (5)); $C$ is a fuzzy set.

b) Functional consequent (Eq. (6)); $p, q$ and $r$ are constants.

$$IF \quad x \ is \ A \quad and \quad y \ is \ B \quad THEN \quad f \ is \ C \tag{5}$$

$$IF \quad x \ is \ A \quad and \quad y \ is \ B \quad THEN \quad f = px + qy + r \tag{6}$$

In general, the fuzzy inference system (FIS) incorporates an expert's experience into the system design through 4 steps or parts; the Knowledge Base, Fuzzifier, Fuzzy Inference Engine and the Defuzzifier (see Fig. 3). The 'fuzzifier' uses the knowledge-base that includes the information given by the experts in the form of linguistic fuzzy rules and transforms the 'crisp' inputs into fuzzy inputs through membership functions representing fuzzy sets of input vectors. The Fuzzy Inference Engine uses them together by a method of reasoning and the 'Defuzzifier' then transforms the fuzzy results of the inference into a crisp output using a de-fuzzification method (Herrera and Lozano 2003).

The knowledge-base comprises two components: a data-base comprising membership functions of the fuzzy sets used in the fuzzy rules, and a rule-base comprising a collection of linguistic rules combined by a specific operator. Fig. 3 shows a generic structure of an FIS. There are two common types of FIS and they vary according to the differences in the specifications of the consequent part of fuzzy rules (Eqs. (5) and (6)). The first uses the inference method proposed by Mamdani in which the rule of consequent is defined by fuzzy sets with the structure of Eq. (5) (Mamdani and Assilian 1975).

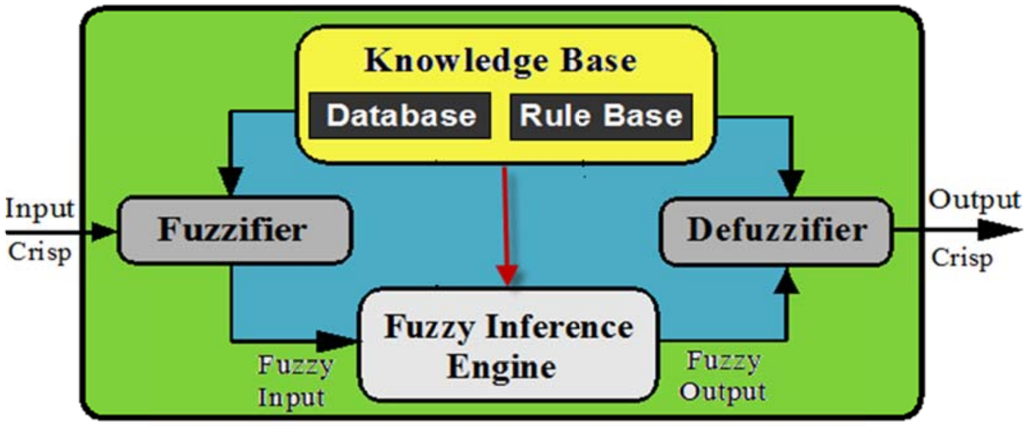


Fig. 3 A flow diagram of a fuzzy inference system (FIS) (Mohammadhassani 2013a)

The second type, namely the TSK system was proposed by Takagi and Sugeno (1985) with an inference engine, where the conclusion of a fuzzy rule consists of a weighted linear combination of the crisp inputs rather than a fuzzy set. The structure of the TSK system is shown in Eq. (6); the TSK models are most suited for approximating large non-linear systems.

The knowledge-base with the database and rule-base of an FIS are constructed from an expert's knowledge. The expert first selects the membership functions and rules whereby fuzzy models help in extracting expert knowledge at a suitable level. Fuzzy systems are also constructed from data which alleviate the problem of knowledge acquisition. Various techniques are used to analyze the data to ensure best possible accuracy. There are two common approaches in constructing an FIS with available data. The first approach is where the rules of a fuzzy system are designated a priori and the parameters of the membership functions are adapted in the learning process from input to output data through an evolutionary algorithm (e.g., genetic algorithm). The second approach is where a fuzzy system is generated using hybrid neural nets. The neural net defines the shape of membership functions of the premises and this architecture-learning procedure is known as the adaptive network-based fuzzy inference system, or in short, the ANFIS (Jang 1993).

#### *2.2.3 Adaptive network-based fuzzy inference system (ANFIS) (Mohammadhassani 2013a)*

As a multilayer feed-forward network, the ANFIS has individual nodes that perform a particular function for incoming signals as well as sets of parameters pertaining to their respective nodes (Jang 1993). The ANFIS is able to map unseen inputs to their outputs by just learning the rules from the data previously seen. A simple structure of this type of network having just two inputs of x and y and one output of $f$ is shown in Fig. 4.

As seen in Fig. 4, the ANFIS architecture contains five layers including Layer 1: Fuzzifier, Layer 2: Product, Layer 3: Normalized, Layer 4: Defuzzifier and Layer 5: Total Output. It should be noted that by using just two membership functions for each of the input data x and y, the general form of a first-order TSK type of fuzzy IF–THEN rule has been given by Eq. (7). Here, when re-written, the rule $i$ of the ANFIS is as follows

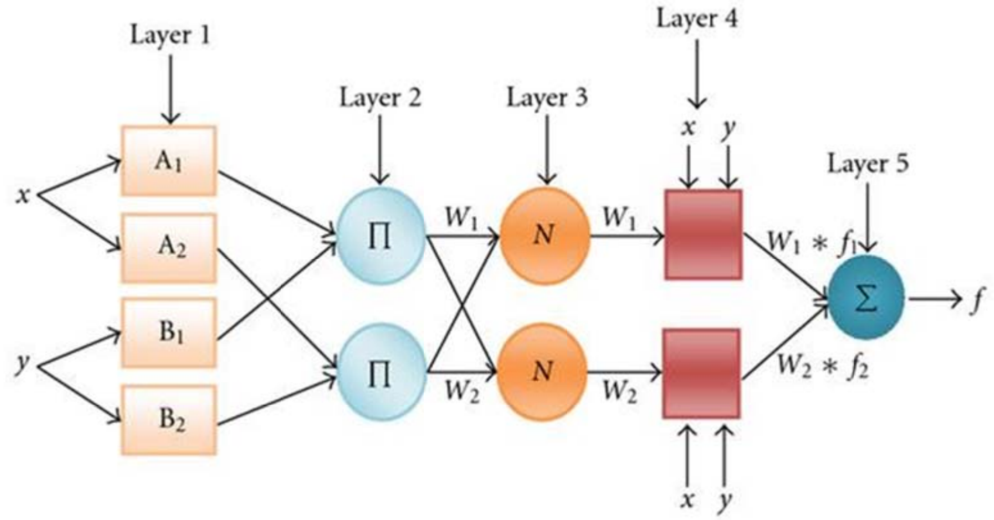


Fig. 4 A simple ANFIS architecture (Mohammadhassani 2013a)

Rule $i$: $IF \quad x \text{ is } A_i \quad and \quad y \text{ is } B_i \quad THEN \quad f_i = p_i x + q_i y + r_i, \quad i = 1,2,...,n$ (7)

where $n$ is the number of rules and $p_i$, $q_i$ and $r_i$ are the parameters identified in the training process. In the early stage of the learning process, the membership function (μ) of each of the linguistic labels $A_i$ and $B_i$ is calculated as follows

$$O_i^1 = \mu_{Ai}(x), \quad i=1,2,\ldots,n \tag{8}$$

$$O_i^1 = \mu_{Bi}(y), \quad i=1,2,\ldots,n \tag{9}$$

In the second layer, namely the Product layer, the previously calculated membership degrees of linguistic variables are multiplied as in Eq. (10)

$$O_i^2 = w_i = \mu_{Ai}(x)\, \mu_{Bi}(y) \quad i=1,2,\ldots,n \tag{10}$$

In the third layer, which is the Normalized layer, the ratio of each weight to the total weights is calculated

$$O_i^3 = \overline{w}_i = \frac{w_i}{\sum_{i=1}^{n} w_i} \quad i=1,2,\ldots,n \tag{11}$$

The fourth layer, which is the Defuzzification layer, has adaptive nodes with outputs that depend on the parameter(s) pertaining to these nodes; the learning rule specifies how these parameters are altered to minimize the prescribed error (Jang 1993). The association of these nodes is as follows

$$O_i^4 = \overline{w}_i f_i = \overline{w}_i(p_i x + q_i y + r_i) \quad i=1,2,\ldots,n \tag{12}$$

Finally in the fifth layer, namely the Total Output, the summation of all the incoming signals is performed and the output is the final result of the system as shown in Eq. (13)

$$O_i^5 = \sum_{i=1}^{n} \overline{w_i}\, f_i i = 1,2,\ldots,n \tag{13}$$

## 3. Results and discussion

The data set was first normalized using the Gaussian normalization technique. 80% of this normalized data was then randomly chosen as the training data and the remainder 20% as the testing data. The ANFIS models with different parameters (total nine) as inputs were implemented using MATLAB version R2010a.

The Genfis2 function based on a subtractive clustering method is used to generate the FIS structures. Finding the best structure with the suitable membership function parameters involves two processes: Learning and Testing. In the Learning process, first off, the membership functions of the inputs are generated using a subtractive clustering and then tuned using a back propagation algorithm combining a recursive least square method. The Testing step follows where the generalization ability of the generated model is checked. To decrease the Mean Square Error (MSE) obtained in this method, the number of membership functions was gradually increased. This was done by lowering the range of influence of cluster centers in a step by step method, and through the trial and error mode.

Linear Regression (LR) is carried out to establish a relationship between the output and input data used in the proposed ANFIS model. LR is simple, yet an excellent and effective method for predicting domains with numeric attributes where the linear models function as building blocks for more complex learning tasks.

MSE and Correlation Coefficient / Pearson Coefficient (R) values are used in this study to evaluate the comparative methods. As a risk function, the MSE corresponds with the expected value of the squared error loss or quadratic loss. R refers to the degree of success in reducing the standard deviation (SD). It is widely used as a measure of the strength of linear dependence between two variables. The MSE calculation is shown in Eq. (1) while R is calculated in Eq. (14) as follows

$$R^2 = 1 - \frac{\sum_{k=1}^{L} (y(k) - \hat{y}(k))^2}{\sum_{k=1}^{L} (y(k) - y_{ave})^2} \tag{14}$$

where $\hat{y}(k)$ , $y(k)$ and $y_{ave}$ are the ANFIS predicted output, the actual / observed output and average actual output respectively; $L$ is the total number of training/testing instances. Table 3 summarizes the MSE and R results obtained using the proposed method and the LR separately using both the training data and testing data.

It is noted that the MSE value from the ANFIS is approximately 76 times smaller for the training set and more than 2 times smaller for the testing set than the values from the LR. The R values from the ANFIS for the testing data is 0.9008 and 0.9979 for the training set, while both are more than the corresponding value in the LR.

Table 3Comparison of MSE and R values in ultimate shear prediction using ANFIS and LR

| | Training Set | | | Testing set | | |
|---|---|---|---|---|---|---|
| Methods | Instances | MSE | R | Instances | MSE | R |
| LR | 111 | 0.3135 | 0.8286 | 28 | 0.4672 | 0.7248 |
| ANFIS | 111 | 0.0041 | 0.9979 | 28 | 0.2058 | 0.9008 |

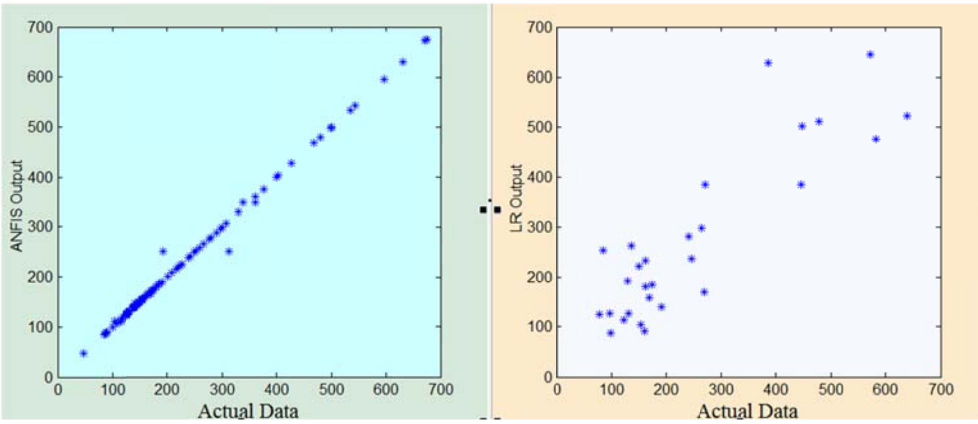

Fig. 5 Ultimate shear prediction performance from (a) ANFIS and (b) Linear regression

To compare the performance of the ANFIS and LR, Fig. 5 shows the ultimate shear prediction performance from the LR and ANFIS for the testing data. The horizontal and vertical axes represent the actual and predicted data, respectively.

A precise modelling would result in a direct linear relation between the actual and predicted data (a line of perfect agreement (i.e., a line at $45^0$). Fig. 5 reveals that the ANFIS method is highly accurate and more precise, compared to the LR for the ultimate shear prediction of deep beams.

Fig. 6 shows the architecture of the proposed ANFIS with nine inputs for it.

After the finding of the best architecture, the predicted results are presented as V*predict* in Table 1. Results suggest the effectiveness of the ANFIS in predicting shear strength of deep beams with this dataset (Fig. 5(a)). The value of variance, correlation coefficient, RMSE and average actual strength to predicted ratio are presented for all specimens for RC deep beam dataset with this approach (Table 4).

The average actual-to-predicted shear strength ratio of all specimens is 0.99 and 0.86 with the ANFIS method and LR, respectively. Another study (Pal and Deswal 2011) with the same target using ACI method, CEB-FIP MC90, Support vector regression (SVR) approaches with polynomial and radial basis kernel function provides the average values of 1.69, 1.74 , 1.28 1.006 and 1.013 respectively in the range of these datasets.

Comparison of these studies confirms the superiority of ANFIS and SVR in shear strength prediction in contrast to other applied methods.

A comparison of the RMSE and correlation coefficient values (Tables 3 and 4) suggests better performance with the ANFIS in comparison to the LR with this dataset.

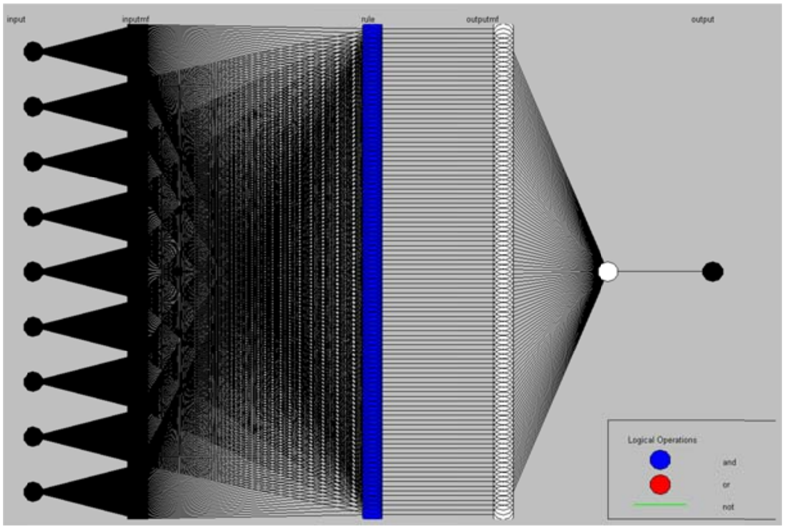


Fig. 6 ANFIS Architecture

Table 4 Average, Variance, Correlation Coefficient, MSE and Coefficient of Variation of different methods with this datasets

| | ANFIS | LR |
|---|---|---|
| AVG | 0.99 | 0.86 |
| VAR | 0.012 | 2.36 |
| CORR | 0.97 | 0.81 |
| CV | 11.01% | 179.07% |
| STDEV | 0.109 | 1.54 |

Fig.7 illustrates the variation of this particular ratio with the L/d ratio.

A large variation in the ratio of actual-to-predicted strength is obtained with the LR method in comparison to the ANFIS method that suggests an improved performance by this approach compared to the LR. In all ranges of the L/d ratios, most of the values are very close to 1 for ANFIS prediction. The variations of the ratio of actual strength to predicted strength with the a/d ratio for both the ANFIS and LR are shown in Fig. 8.

Results indicate a better performance by the ANFIS for all ranges of $a/d$ values considered in this study in comparison to the LR method.

The compressive strength of the concrete ( $f_c'$) was plotted against the ratio of the actual strength to predicted strength and this is shown in Fig. 9 for the ANFIS and LR.

Result indicates that the Strength predications by the ANFIS are mostly unaffected by the variation in the compressive strength of concrete and performed better than the LR method.

Figs. 7-9 indicate an improved performance by the ANFIS for deep beam strength prediction in comparison with the LR.

The relation between the input and output variables is visualized with modelled fuzzy surfaces shown in Figs. 10-12. The Graphical User Interface (GUI) tool allows the examining of the output surface of an FIS model to be executed. The GUI provides a fast 3-D output visual impression of possible combinations of the two input variables to analyse and predict the ultimate shear strength in deep beams. The FIS allows mathematical solutions in determining the ultimate shear strength of deep beams, based on data such as the compressive strength of concrete versus shear span-depth ratio; the horizontal web reinforcement ratio versus vertical web reinforcement ratio and the horizontal web reinforcement ratio versus shear span-depth ratio.

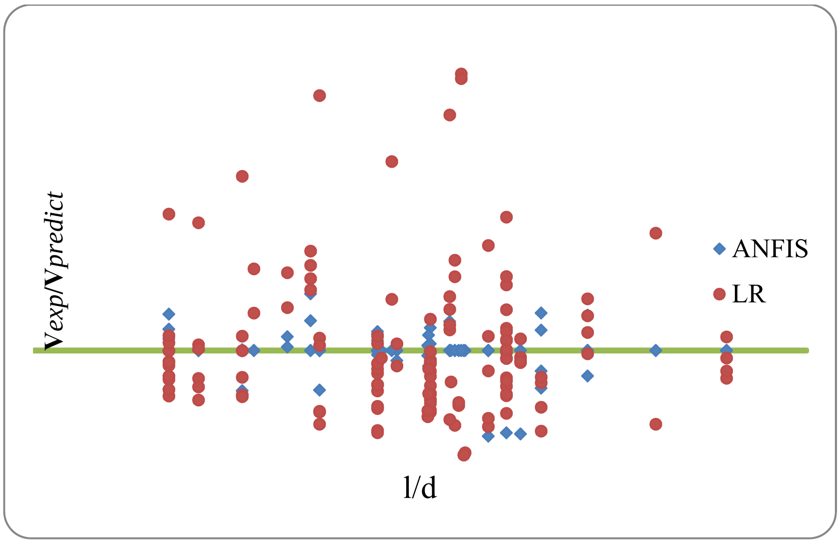


Fig. 7 Variation of actual to predicted shear strength with $l/d$ using ANFIS and LR methods

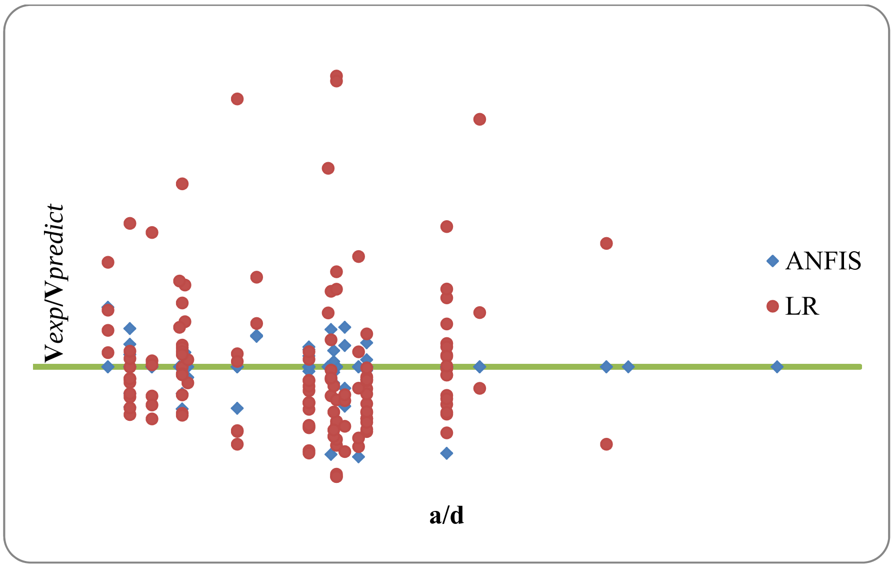


Fig. 8 Variation of actual to predicted strength with $a/d$ using ANFIS and LR methods

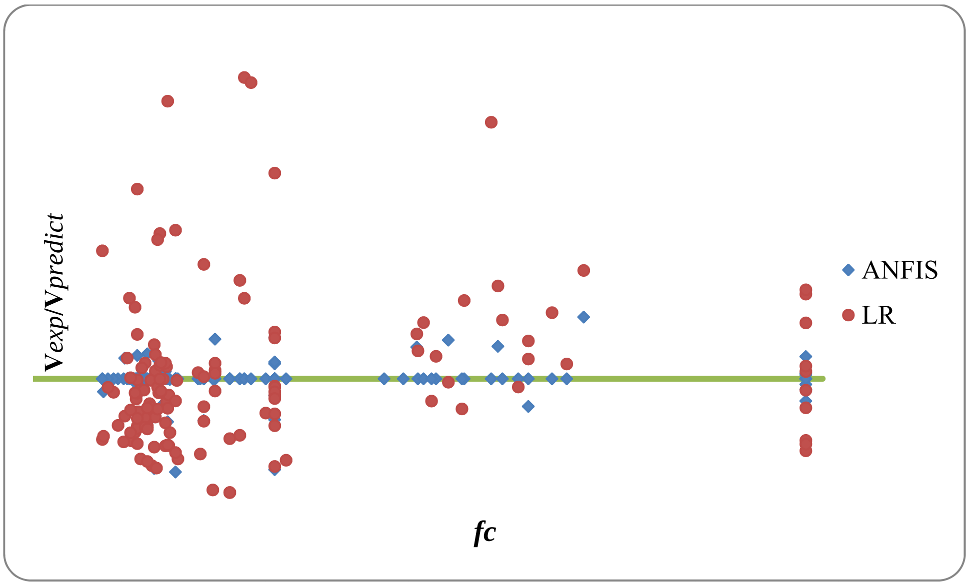


Fig. 9 Variation of actual to predicted shear strength with $f_c'$ using ANFIS and LR methods

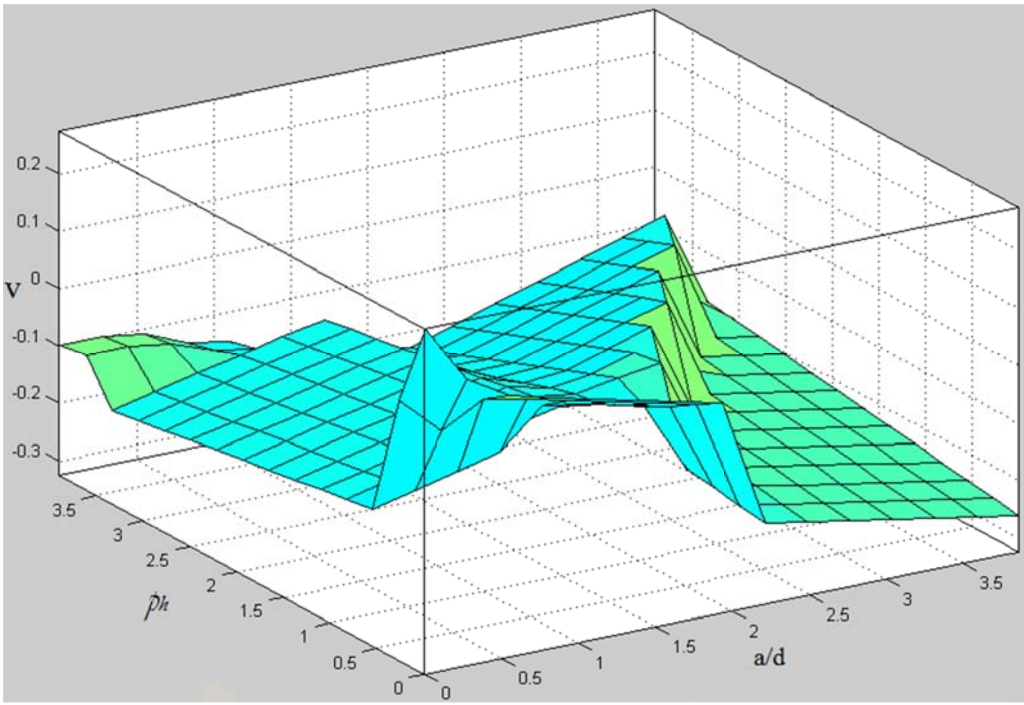


Fig. 10 Fuzzy surface: Horizontal web reinforcement ratio versus shear span-depth ratio in ultimate shear strength prediction

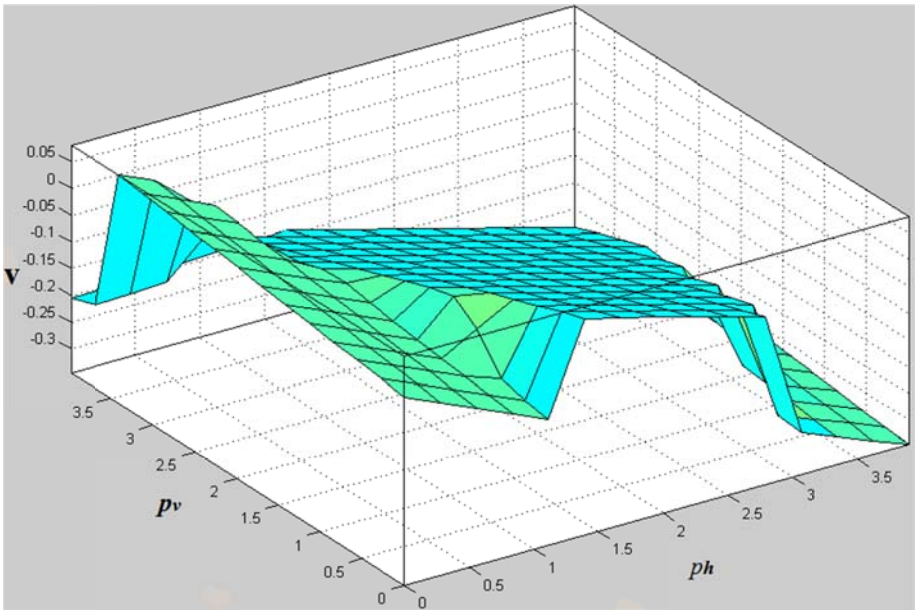


Fig. 11 Fuzzy surface: Horizontal web reinforcement ratio versus vertical web reinforcement ratio in ultimate shear strength prediction

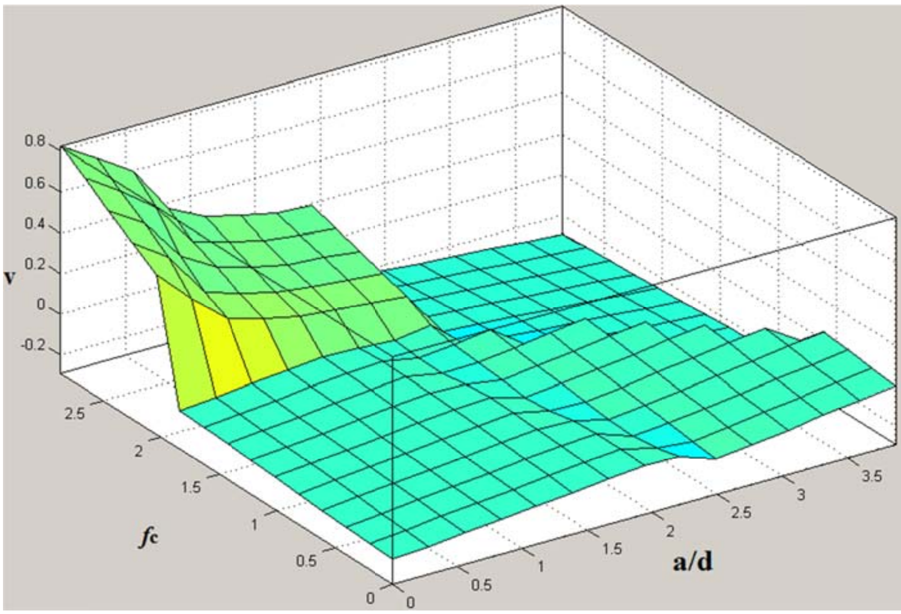


Fig. 12 Fuzzy surface: Compressive strength of concrete versus shear span-depth ratio in ultimate shear strength prediction

Table 5 Sensitivity analysis of input variables using ANFIS

| Omitted input parameter | | $l/d$ | $d/b_w$ | $a/d$ | $f_c'$ | $f_{yh}$ | $f_{yv}$ | $\rho_h$ | $\rho_s$ | $\rho_v$ |
|---|---|---|---|---|---|---|---|---|---|---|
| Evaluation of remained parameters | MSE | 0.34 | 0.30 | 0.53 | 0.64 | 0.37 | 0.45 | 0.26 | 0.70 | 0.26 |
| | R | 0.82 | 0.84 | 0.69 | 0.66 | 0.80 | 0.74 | 0.86 | 0.66 | 0.87 |

Fig. 12 confirms the increase in shear strength of deep beams with the increase in the concrete compressive strength and the decrease in the shear span to depth ratio.

The input-output surfaces shown in Figs. 10-12 are nonlinear and monotonic surfaces that illustrate how an ANFIS model responds to varying values in the prediction of ultimate shear strength.

### *3.1 Sensitivity Analysis (S.A)*

This section discusses the utilisation of the ANFIS in judging the importance of input parameters (i.e., $l/d$, $d/b_w$, $a/d$, $f_c$, $f_{yh}$, $f_{yy}$, $\rho_h$, $\rho_s$, $\rho_v$) on the shear strength prediction of deep beams. To rank different input parameters on shear strength prediction of deep beams, the procedure involves deleting one input from the dataset and using the resultant dataset to test and train the model using the ANFIS and for the ANFIS to be evaluated in terms of its MES and R. For this purpose, the input omission and results are provided in Table 5.

Results from Table 5 suggest that the shear span to depth ratio ($a/d$) and concrete cylinder strength ($f_c'$) have major influence on the shear strength prediction of deep beams, that is confirmed with the SVR in another study (Pal and Deswal 2011).

## 4. Conclusions

The applications of the Adaptive Network-Based Fuzzy Inference System (ANFIS) and linear regression (LR) models in the prediction of ultimate shear strength for deep beams have been demonstrated in this study.

This study proposes the ANFIS as a powerful computational tool that can effectively be used to analyse the complex relationship formed between various parameters used in predicting the shear strength of deep beams.

The ANFIS has relatively higher accuracy and precision compared to the LR. The MSE from the ANFIS is approximately 76 times lesser for the training set and more than two times lesser for the testing set and therefore, conclusively, the ANFIS is more accurate and effective than the LR in terms of its prediction of the ultimate shear strength in reinforced concrete deep beams.

The parametric study verifies the increasing shear strength of deep beams with an equal increase in the concrete strength and decrease in the shear span to- depth-ratio.

The sensitivity analysis (S.A) shows that the shear span to depth ratio ($a/d$) and the concrete cylinder strength ( $f_c'$ ) have major influence on the shear strength prediction of deep beams.

## Acknowledgments

"Support for this research was provided by University of Malaya Research Grant (UMRG), Project Number: PR004D-13AET. This support is gratefully acknowledged".

## References

Akib S., Mohammadhassani M. and Jahangirzadeh A. (2014), "Application of ANFIS and LR in prediction of scour depth in bridges", *Comput. Fluids*., **91**, 77-86.

Akrami S.A., El-Shafie A. and Jaafar O. (2013), "Improving rainfall forecasting efficiency using modified adaptive neuro-fuzzy inference sSystem (MANFIS)", *Water Resour. Manag*., **27**(9), 3507-3523.

Bilgehan, M. (2011), "Comparison of ANFIS and NN models-with a study in critical buckling load estimation", *Appl. Soft Comput*., **11**(4), 3779-3791.

Braestrup M.W. and Nielsen M.P. (1983), *Plastic methods of analysis and design*, In Handbook of Structural Concrete, London, Pitman.

CIRIA Guide 2. (1977), *Construction Industry research and Information association. the design of deep beams in reinforced concrete*, Ove Arup & Partners London.

Herrera, F. and Lozano, M. (2003), "Fuzzy adaptive genetic algorithm: design, taxonomy, and future directions", *Soft Comput*., **7**(8), 545-562.

Jang, J.S.R. (1993), "Adaptive network based fuzzy inference system", *IEEE T. Syst., Man Cy.*, **23**, 665-685.

Kao, C.Y. and Hung, S.L. (2003), "Detection of structural damage via free vibration responses generated by approximating artificial neural networks", *Comput. Struct.*, **81**(28-29), 2631-2644.

Khaleie, S. and Fasanghari, M. (2012), "An intuitionistic fuzzy group decision making method using entropy and association coefficient", *Soft Comput*., **16**(7), 1197-1211.

Kong, F., Robins, P. and Cole, D. (1970), "Web reinforcement effects on deep beams", *ACI Struct. J*., **67**(12), 1010-1017.

Lin, C.T., Lin, C.T. and Lee, C.S.G. (1996), *Neural fuzzy systems: a neuro-fuzzy synergism to intelligent systems*, Prentice Hall PTR, 797.

Lu, W.Y., Hwang, S.J. and Lin, I.J. (2010), "Deflection prediction for reinforced concrete deep beams", *Comput. Concrete*, **7**(1), 1-16.

Mamdani, E. and Assilian, S. (1975), "An experiment in linguistic synthesis with a fuzzy logic controller", I*nt. J. Man. Mach. Stud*., **7**(1), 1-13.

Mashrei, M.A., Abdulrazzaq, N., Abdalla, T.Y. and Rahman, M.S. (2010), "Neural networks model and adaptive neuro-fuzzy inference system for predicting the moment capacity of ferrocement members", *Eng. Struct*., **32**(6), 1723-1734.

Mohammadhassani, M., Jumaat, M.Z., Jameel, M., Badiee, H. and Arguman, A. (2011), "Ductility and performance assessment of high strength self compacting concrete (HSSCC) deep beams an experimental investigation", *Nucl. Eng. Des*., **241**, 2060-2067.

Mohammadhassani, M., Jumaat, M.Z., Ashour, A. and Mohameed, J. (2011a), "Failure modes and serviceability of high strength self compacting concrete deep beams", *Eng. Fail. Anal*., **18**(8), 2272-2281.

Mohammadhassani, M., Nezamabadi-Pour, H., Jumaat, M.Z., Jameel, M. and Arumugam, A.M.S. (2013), "Application of Artificial Neural Network (ANN) and Linear Regressions (LR) in predicting the deflection of concrete deep beams", *Comput. Concrete*., **11**(3).

Mohammadhassani, M., Nezamabadi-Pour, H., Jumaat, M.Z., Jameel, M., Hakim, S.J.S. and Zargar, M. (2013a), "Application of the ANFIS model in deflection prediction of concrete deep beam", *Struct. Eng.*

*Mech*., **45**(3), 319-332.

Möller, B., Liebschera, M., Schweizerhofb, K., Matternb, S. and Blankenhornb, G. (2008), "Structural collapse simulation under consideration of uncertainty - Improvement of numerical efficiency", *Comput. Struct*., **86**(19-20), 1875-1884.

Nielsen, M.P. (1971), "On the strength of reinforced concrete discs. copenhagen, acta polytechnica scandinavica", Civil Engineering and Building Construction Series.

Oh, J.K. and Shin, S.W. (2001), "Shear strength of reinforced high strength concrete deep beam", *ACI Struct. J*., **8**, 164-173.

Pal, M. and Deswal, S. (2011), "Support vector regression based shear strength modelling of deep beams", *Comput. Struct*., **89**(13-14), 1430-1439.

Sanad, A. and Saka, M.P. (2001), "Prediction of ultimate strength of reinforced concrete deep beams by neural networks", *J. Struct. Eng. - ASCE*, **127**(7), 818-828.

Smith, K.N. and Vantsiotis, A.S. (1982), "Shear strength of deep beams", Amarican concrete institute (ACI), **79**, 201-213.

Takagi, T. and Sugeno, M. (1985), "Fuzzy identification of systems and its applications to modeling", *IEEE T. Syst. Man Cy*., **35**, 116-132.

Tan, K., Kong, F., Teng, S. and Guan, L. (1995), "High-strength concrete deep beams with effective span and shear span variations", *ACI Struct. J*., **92**(4), 395-405.

Tan, K., Kong, F., Teng, S. and Weng, L. (1997), "Effect of web reinforcement on high-strength concrete deep beams", *ACI Struct. J*., **94**(5), 572-582.

Tan, K. and Lu, H. (1999), "Shear behavior of large reinforced concrete deep beams and code comparisons", *ACI Struct. J*., **96**(5), 836-845.

Yang, K.H., Chung, H.S., Lee, E.T. and Eun, H.C. (2003), "Shear characteristics of high-strength concrete deep beams without shear reinforcements", *Eng. Struct*., **25**(10), 1343-1352.

Yang, K., Eun, H., Lee, E. and Chung, H. (2006), "The influence of web openings on the structural behaviour of reinforced high-strength concrete deep beams", *Eng. Struct*., **28**(13), 1825-1834.

Zadeh, L.A. (1965), "Fuzzy sets. Inform Control", **8**, 338-353.

Zhang, N. and Tan, K.H. (2007), "Size effect in RC deep beams: Experimental investigation and STM verification", *Eng. Struct*., **29**(12), 3241-3254.

*CC*